Available online at www.sciencedirect.com
ScienceDirect
Biochimica et Biophysica Acta 1769 (2007) 514–524
Biochimica et Biophysica Acta BBA
www.elsevier.com/locate/bbaexp

Cloning, genomic organization, and tissue-specific expression of the *RASL11B* gene

Katrin Stolle [a,b], Michael Schnoor [a,b], Georg Fuellen [c,d], Michael Spitzer [c,d], Paul Cullen [a], Stefan Lorkowski [a,b,*]

[a] *Leibniz Institute of Arteriosclerosis Research, University of Münster, Germany*
[b] *Institute of Biochemistry, University of Münster, Germany*
[c] *Bioinformatics Research Group, Department of Medicine and Institute for Evolution and Biodiversity, Department of Biology, University of Münster, Germany*
[d] *Institute for Mathematics and Computer Science, University of Greifswald, Germany*

Received 28 March 2007; received in revised form 25 May 2007; accepted 29 May 2007
Available online 6 June 2007

Abstract

RASL11B is a member of the small GTPase protein family with a high degree of similarity to RAS proteins. Cloning of RASL11B mRNA and *in silico* analyses revealed that the human *RASL11B* gene spans about 4.5 kb and comprises four exons on chromosomal locus 4q12. The proximal 5′-flanking region of the gene lacks a TATA box but is GC-rich and contains a CCAAT box and several Sp1 sites. Consistent with this, the *RASL11B* gene was found to be expressed in all tissues investigated, with highest levels in placenta and in primary macrophages. The predicted RASL11B protein has no typical prenylation signal, indicating that it is probably not anchored to cellular membranes. RASL11B was induced during maturation of THP-1 monocytic cells into macrophage-like cells and in coronary artery smooth muscle cells after treatment with TGF-β1. These results indicate that RASL11B may play a role in TGF-β1-mediated developmental processes and in pathophysiologies such as inflammation, cancer, and arteriosclerosis.

Keywords: RASL11B; RASL11A; RAS-like protein; GTPase; Transforming growth factor β1; TGF-β1; Smooth muscle cell

1. Introduction

Members of the RAS protein family have been found in all eukaryotes investigated and they modulate a wide variety of cellular processes ranging from cell growth, organization of the cytoskeleton, and intracellular traffic to cell survival and apoptosis [1,2].

The human RAS protein family comprises more than 150 members and forms a subfamily of the protein family of small monomeric GTPases. The family of RAS proteins itself is divided into five different major subfamilies named RAS, RHO, RAB, ARF, RAN and other proteins belonging to the RAS family [3]. All RAS proteins have different intracellular localizations and interact with different effectors, but all share a so-called G-domain which is essential for the binding and hydrolysis of GTP [4].

Typically, RAS proteins are post-translationally modified by prenylation at the CAAX signal located at the end of their C-terminus. Addition of a farnesyl or geranylgeranyl group to this motif allows anchoring of the RAS protein to cellular membranes [5].

RAS-like GTPases form a poorly characterized and heterogeneous subfamily of the small monomeric GTPase protein family. Most of them are allocated to the RAS subfamily even though they lack some of the characteristics of these proteins such as the prenylation signal (e.g., RIT1 and RIT2) or the effector domain (e.g., RHEB2, RASD2, ARHI, NKIRAS1 and NKIRAS2) [6].

* Corresponding author. Leibniz-Institut für Arterioskleroseforschung, Domagkstraße 3, 48149 Münster, Germany. Tel.: +49 251 83 52072; fax: +49 251 83 52062.
E-mail address: stefan.lorkowski@uni-muenster.de (S. Lorkowski).

0167-4781/$ - see front matter © 2007 Elsevier B.V. All rights reserved.
doi:10.1016/j.bbaexp.2007.05.005

In the present study, we cloned the small RAS-like GTPase RASL11B (RAS-like protein, family 11, member B) in order to investigate the organization of the *RASL11B* gene. We analyzed the expression of RASL11B during macrophage maturation and the tissue-specific expression of the *RASL11B* gene. A further aim of this study was to characterize the influence of TGF-β1 on the expression of RASL11B in coronary artery smooth muscle cells (caSMCs). In addition, we analyzed the expression of the *RASL11A* gene encoding the previously described RASL11A protein with unknown function [7], which is the closest human homologue of RASL11B.

2. Materials and methods

2.1. Cell culture

Human caSMCs were purchased from BioWhittaker (Walkersville, MD). Cells were cultured using the SmGM2 Bullet Kit in medium containing 5% fetal bovine serum (BioWhittaker) as previously described [8]. When 80% confluent, cells were grown for 48 h in MCDB 131 medium (Sigma-Aldrich Chemie, Taufkirchen, Germany) supplemented with 100 units/ml penicillin, 100 μg/ml streptomycin and 4 mM L-glutamine (ICN Biomedicals, Eschwege, Germany), 100 mM sodium hydrogen carbonate (Sigma-Aldrich Chemie), 10 μl/ml ITS (BD Biosciences, Heidelberg, Germany), 30 μg/ml heparin (Merckle, Ulm, Germany), 50 μg/ml ascorbic acid (Sigma-Aldrich Chemie) and 1% fetal bovine serum (CytoGen, Sinn-Fleisbach, Germany). Using the supplemented MCDB 131 medium, cells were incubated with or without 10 ng/ml TGF-β1 for different times as indicated in the figures. The THP-1 monocytic cell line was purchased from the American Tissue Culture Collection (Rockville, MD). The cells were maintained in RPMI 1640 containing L-glutamine, 10% fetal calf serum (PAA Laboratories, Pasching, Germany), and 0.1 mg/ml penicillin/streptomycin/L-glutamine solution (Invitrogen, Karlsruhe, Germany). THP-1 monocytes were harvested directly from the cell suspension or seeded and differentiated into macrophages using 0.1 mM phorbol 12-myristate 13-acetate (PMA; Sigma-Aldrich Chemie) and 50 nM 2-mercaptoethanol (Sigma-Aldrich Chemie) for 4 days as previously described [9].

2.2. RNA isolation

Total cellular RNA was isolated using the RNeasy Mini kit (Qiagen, Hilden, Germany) as described [10]. Contaminating genomic DNA was removed using DNase I (Qiagen).

2.3. Reverse transcription

Five micrograms of total RNA were reverse transcribed using 500 ng/μl oligo(dT) primer (Invitrogen), 1 mM dNTPs (Fermentas, St. Leon-Rot, Germany), 20 units of ribonuclease inhibitor (Promega, Mannheim, Germany) and 200 units of M-MuLV reverse transcriptase RevertAid (Fermentas) in a total volume of 20 μl as previously described [11]. After diluting the cDNA tenfold, aliquots were immediately used or stored at −20 °C.

2.4. RACE assays

RACE analyses were performed using the GeneRacer Kit (Invitrogen) and different reverse or forward primers specific for the human RASL11B mRNA (Table 1). For 5′-RACE assays, 1 μg of total RNA isolated from human caSMCs was incubated with calf intestinal phosphatase in order to eliminate truncated non-mRNAs and mRNAs. The dephosphorylated mRNA was treated with tobacco acid pyrophosphatase to remove the 5′-cap. The full-length mRNA was ligated to the GeneRacer RNA oligonucleotide using T4 RNA ligase. After reverse transcription using the GeneRacer oligo(dT) primer, PCRs were performed using the GeneRacer 5′-forward primer and different RASL11B-specific reverse primers (Table 1). Nested PCRs were performed using the GeneRacer 5′-nested forward primer and nested RASL11B-specific reverse primers (Table 1). For 3′-RACE analyses, 1 μg of total RNA isolated from human caSMCs was reverse transcribed using the GeneRacer oligo(dT) primer. PCRs were performed using the GeneRacer 3′-reverse primer and different RASL11B mRNA-specific forward primers (Table 1). Nested PCRs were performed using the GeneRacer 3′-nested reverse primer and nested RASL11B-specific forward primers (Table 1). PCR products were checked on agarose gels and subjected to sequencing.

Table 1
Primers used in this study (PCR and RACE primers were also used for sequencing)

Primer	Sequence	Exon
5′-RACE A reverse	5′-CAG CTT TGT TGG CCA CGA CCA CCA CA-3′	4
5′-RACE B reverse	5′-TGC TGG TGG AGC TGG CTG ATG AGT TCA-3′	4
3′-RACE A forward	5′-CAT GTG CAC CAT CGC CGA GTA CCC C-3′	1
3′-RACE B forward	5′-TTC TCC AGT CCC TCA GTC CCT TCC CGC-3′	1
3′-RACE C forward	5′-ACA CTC CAG GTA TTC AGG TCC-3′	3
Real-time PCR forward	5′-ACA CTC CAG GTA TTC AGG TCC ATG-3′	3
Real-time PCR reverse	5′-ACA GCA TCT GCC CAG CGA-3′	4
Splicing intron 1 forward	5′-ACC ATC GCC GAG TAC CCC-3′	1
Splicing intron 1 reverse	5′-GAA TCG TTT GGT GAG GAA CCG-3′	2
Splicing intron 2 forward	5′-CCG GTT CCT CAC CAA ACG A-3′	2
Splicing intron 2 reverse	5′-GAG TGT CTT GAA CCT GAA GAG CCA-3′	3
Splicing intron 3 forward	5′-GTT CAG ATA GAA GGT GAA ACC CTG G-3′	3
Splicing intron 3 reverse	5′-TGG AAG GCG CTG TAG ACA TCA-3′	4
Sequencing 1 forward	5′-AGT CTG GGT CTG GAG CCT G-3′	1
Sequencing 2 forward	5′-TAG GCC TGG CTG AGT TGT GC-3′	4b
Sequencing 1 reverse	5′-TGG AAG GCG CTG TAG ACA TCA-3′	4
Sequencing 2 reverse	5′-CTG GCC CAT AAA CTC AAC C-3′	4b

2.5. DNA sequencing

DNA sequencing was performed using the BigDye 2.0 or 3.1 Terminator Cycle Sequencing kit (Applied Biosystems, Weiterstadt, Germany) in a PTC-200 thermal cycler (MJ Research, Waltham, MA) as described [11]. PCR products for sequencing were either gel purified and/or cloned into pCRII-TOPO vector (Invitrogen) using the TOPO TA Cloning kit (Invitrogen). The primers used for sequencing PCR products were identical to the primers used for amplification of corresponding targets. Sequencing of PCR fragments cloned into pCRII-TOPO vector was performed using M13/pUC reverse and M13/pUC forward primers (Invitrogen). Products of the sequencing reaction were purified by gel filtration using Sephadex G-50 Superfine (Amersham Biosciences, Munich, Germany) prior to electrophoretic separation and fluorimetric detection on an ABI Prism 3700 DNA sequencer (Applied Biosystems).

2.6. Primer design

PCR primers for real-time RT-PCR (Table 1) were designed using the Primer Express v2.0.0 software (Applied Biosystems) as previously described [8]. Primers were purchased from Invitrogen and forward and reverse primers locate in different exons.

2.7. RT-PCR

RT-PCR mixes of 20 μl included 0.5 μl cDNA, 1.25 units HotStar *Taq* polymerase and PCR buffer (both from Qiagen) containing 1.5 mM $MgCl_2$. In some cases, $MgCl_2$ up to 3.5 mM was added. PCR cycling conditions were as follows: Initial denaturation at 95 °C for 10 min, followed by 40 cycles of 15 s at 95 °C, 30 s at the primer melting temperature and 72 °C for 1 min per 1000 base pairs. Products were checked by agarose gel electrophoresis and identity of PCR products was verified by sequencing.

2.8. Real-time RT-PCR

We performed real-time RT-PCR assays using the ABI PRISM 7900HT Sequence Detection System (Applied Biosystems) and the QuantiTect SYBR-Green PCR kit (Qiagen). Cycling parameters were: initial denaturation at 95 °C for 10 min, followed by 40 cycles of 15 s at 95 °C and 60 s at 60 °C. Each reaction contained cDNA corresponding to between 0.2 and 7 ng total RNA and 200 nM of forward and reverse primer (Table 1). For tissue-specific mRNA expression analyses, total RNA of different tissues was obtained from Clontech (Saint-Germain-en-Laye, France) or Ambion (Darmstadt, Germany). Five micrograms of each total tissue RNA were reverse transcribed as described above. For each assay, cDNA samples were assayed in duplicates at least two times and analyzed using the Sequence Detection System v2.1 software (Applied Biosystems). We performed relative mRNA quantification using the ΔΔCt method and normalized samples as follows. In case of tissue-specific mRNA expression analyses, fold changes were finally normalized to the three most stably expressed housekeeping genes, 14 kDa signal recognition particle (SRP14; NM_003134), DNA directed RNA polymerase II polypeptide K (NM_005034) and family 3A histone H3 (NM_002107), using GeNorm [12]. All relative expression levels in tissues were calculated using RASL11B expression in bone marrow RNA (showing lowest abundance of RASL11B mRNA) and RASL11A expression in endothelial cells (showing lowest abundance of RASL11A mRNA) as references. For the remaining real-time RT-PCR analyses, RNA was isolated from at least two different experiments and cDNA synthesis was performed at least two times for every RNA sample using 5 μg of total RNA as described above. Real-time RT-PCR was performed in duplicates at least three times for every time point and fold changes were normalized to the expression of the housekeeping gene SRP14, expression of which was not affected by TGF-β1 (data not shown). For TGF-β1 dependent expression analyses, PCR efficiencies were calculated using cDNA dilutions derived from human caSMCs and taken into account. Following PCR amplification, samples were subjected to melting temperature analyses. The identity of PCR products was verified by sequencing. Controls containing all constituents but the template were performed to rule out contamination of reagents.

2.9. Database searches and multiple sequence alignments

GenBank entry NM_023940 containing the putative human RASL11B mRNA sequence was used to search the GenBank databases to generate an aligned RASL11B mRNA/EST (expressed sequence tag) dataset using BLAST algorithm with standard parameters. Human sequences showing a reasonable number of matching nucleotides to the putative human RASL11B mRNA sequence were extracted. Single nucleotide insertions as well as regions of low quality were removed from each entry using human chromosome 4 sequence (NT_022853.14; 20 February 2007) as reference. Expressed sequence tags in the wrong orientation were made reverse complementary. Sequences not spanning at least one intron were removed as being likely to represent DNA contaminations. A multiple alignment of the processed sequences was generated using DIALIGN with standard options for nucleotide sequence alignments [13] and visualized using VisCoSe [14]. The locations and sizes of exons and introns were extracted by BLAST-based comparison of the consensus of the alignment to the reference sequence of human chromosome 4.

2.10. Sequence retrieval and phylogenetic inference

The RASL11 phylogenetic tree was built by employing the RiPE pipeline [15,16] with an alignment of primate RASL11 protein sequences (NP_076429, NP_996563, XP_001089688, ENSMMUP00000010385, ENSPTRP00000027621, ENSPTRP00000053604) as the starting point (jumpstart alignment) of a PSI-BLAST search [17]. Search results were processed by RiPE, and full length sequences corresponding to hit sequences were retrieved automatically. The full length sequences were aligned by MAFFT using the E-INS-i strategy [18]. The retrieved RASL11 protein data set contained several predicted sequences of questionable quality so that manual filtering was performed. As a consequence, some predicted RASL11 homologous protein sequences were excluded from the phylogenetic analysis for the following reasons (although trees including these sequences show similar topology; data not shown): RASL11C protein sequences of *Oryzias latipes* (ENSORLP00000011944), *Tetraodon nigroviridis* (GSTENG00005626001), *Takifugu rubripes* (NEWSINFRUP00000174682) contain probably mis-predicted exons which were not part of any other RASL11 protein. Further, no experimental data is available supporting reliability of the mis-predicted exons. *Danio rerio* RASL11C protein sequence (NP_001017840.1) shows insufficient homology to other RASL11 proteins within the C-terminal half. RASL11B protein sequences of *Loxodonta africana* (ENSLAFP00000006861) and *Dasypus novemcinctus* (ENSDNOP00000003331) as well as *Loxodonta africana* RASL11A protein sequence (ENSLAFP00000003061) were incomplete. *Macaca mulatta* RASL11A protein sequence (ENSMMUP00000010358) was manually curated. The N-terminal peptide MVAVSSGSGPRSRSPAERLEPQAASSPANRTASAIVSSAASAPAPPVSSGKGRRRGGAGAAAALPGAPSPLKAAGLDSCAGSRRGPGLLVPLSQLAIRLRVRRGPVCSACAPDRGTRSMR was removed because it is not part of any other RASL11 homologous protein. Alignment analyses revealed that the *Rattus norvegicus* RASL11A protein sequence (NP_001002829.1) contains a C-terminus that is probably wrong. Thus, the rat RASL11A protein sequence was manually curated by comparing the mouse RASL11A protein sequence to the rat genome. The N-terminal peptide MGTLRSYNGGEKEGEWGYPGDTQKYEEKKSWNLTSDVKGVVEVKEDSQDLGYS of the rat RASL11A protein sequence was therefore changed to MRPLTMSGHFLLAPIPESSSDYLLPK. Neighbor-Joining by QuickTree [19] was then employed with 1000 bootstrap replicates. Trees based on Bayesian inference [20,21] and Maximum Likelihood [22] were slightly less congruent with the species tree (data not shown). The phylogenetic tree was visualized using NJplot [23].

2.11. In silico analysis of predicted protein sequences and core promoter sequence

Predicted amino terminal protein sequences were analyzed for the presence of signal peptides, the position of cleavage sites and cellular localization using SignalP (http://130.225.67.199/services/SignalP/index.html) [24], the NCBI Conserved Domain Database (http://www.ncbi.nlm.nih.gov/Structure/cdd/cdd.shtml), SMART (http://smart.embl-heidelberg.de/) [25], and PSORT II (http://psort.ims.u-tokyo.ac.jp/) [26]. The core promoter of the human RASL11B gene was analyzed using the Transcription Element Search System (TESS; http://www.cbil.upenn.edu/tess/) [27], MatInspector (http://www.genomatix.de/products/MatInspector/index.html) [28], and Mapper (http://bio.chip.org/mapper) [29] using standard parameters.

2.12. Sequence alignments

For sequence alignments, homologues of RASL11B were identified as described above using only the NCBI GenBank reference sequence (RefSeq) database. The retrieved sequences of homologues of the human RASL11B protein (obtained from *Mus musculus*, *Rattus norvegicus*, *Danio rerio*, *Bos taurus*, and *Xenopus tropicalis*) as well as of the human RASL11A protein (*Mus musculus* and *Rattus norvegicus*) were aligned using CLUSTALW 1.82 (http://www.ch.embnet.org/software/ClustalW.html) and were formatted using ESPript 2.2 (http://espript.ibcp.fr/ESPript/cgi-bin/ESPript.cgi) [30]. The rat RASL11A protein sequence (NP_001002829.1) was manually curated as described above. Calculation of identity and similarity was performed by using the NCBI BLAST 2 Sequences tool using standard settings without using the filter function (http://www.ncbi.nlm.nih.gov/blast/bl2seq/bl2.html).

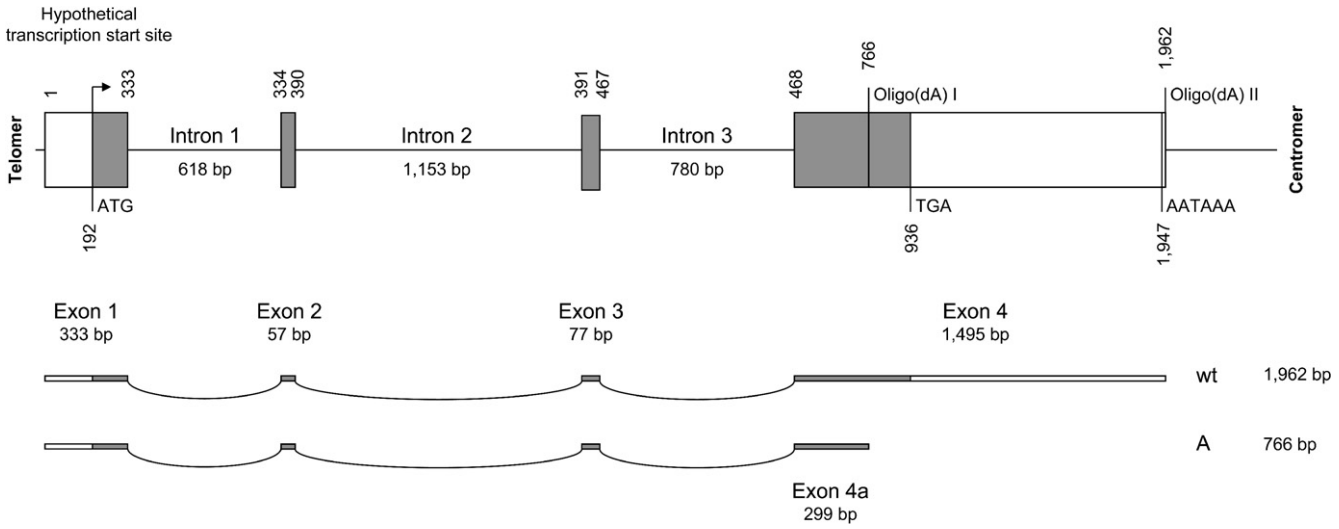

Fig. 1. Schematic representation of the human RASL11B mRNAs and of the genomic organization of the human *RASL11B* gene. RACE and RT-PCR assays revealed four exons encoding a transcript with a total length of 1962 bp (see also Fig. 2). The wild-type transcript is 9 bp longer than the GenBank reference transcript (entry NM_023940). One shorter splice variant (named A) with a length of 766 bp was found. The ATG start and TGA stop codons are located in exons 1 and 4, respectively. The RASL11B open reading frame is shown in grey. The exact positions of exons and introns are listed in Table 2.

2.13. Calculation of conserved sequence motifs

Consensus sequences of the known RASL11 proteins and of each RASL11 subfamily cluster shown in the Supplemental Data were calculated and visualized using VisCoSe (http://viscose.ifg.uni-muenster.de) [14].

3. Results

3.1. Messenger RNA sequence, genomic organization and alternative splicing

RACE assays were performed to identify the 1962 bp of the human RASL11B mRNA and to predict the genomic structure of the human RASL11B gene (Fig. 1). The full-length RASL11B mRNA is 9 bp longer at the 5′-end compared to the sequence originally published in the public NCBI database. 3′-RACE revealed an additional RASL11B transcript with a 3′-end 170 bp shorter than the coding sequence of the full-length wild-type RASL11B transcript. Overall, the human RASL11B gene spans about 4.5 kb on chromosome 4q12 and comprises four exons encoding at least two different transcripts. The positions and sizes of exons and introns are listed in Table 2. The smallest exon of the wild-type RASL11B transcript is exon 2 with 57 bp and exon 4 is the largest with 1495 nucleotides. Sizes of introns range between 618 bp (intron 1) and 1153 bp (intron 2). All splice sites of the wild-type transcript have canonical boundaries [31], starting the intron with ‘gt’ and ending with ‘ag’. Sequences of the different RASL11B transcripts identified in this study have been submitted to the GenBank database (entries AY839725 and AY839726).

3.2. Predicted protein sequence, signal peptides and membrane topology

The wild-type RASL11B transcript encodes a putative protein of 248 amino acids with the open reading frame starting at nucleic acid position 192 in exon 1 and the stop codon at nucleic acid position 936 in exon 4 (see Figs. 1 and 2A). According to SMART, the protein forms a characteristic RAS GTPase domain (PFAM domain entry PF00071) with the typical topology of a six-stranded β-sheet surrounded by five α-helices [32]. According to PSORTII, the RASL11B protein has a putative cleavage site at position 20 but contains no N-terminal signal peptide. The amino acid sequence is mostly

Table 2
Positions of the exons comprising the human 4.5 kb *RASL11B* gene on chromosomal locus 4q12

Exon	Exon size (bp)[a]	Position[a]	Intron size (bp)[a]	Splice acceptor site[a]	Donor acceptor site[a]
				intron′EXON	EXON′intron
1	333	1,068,367–1,068,699	618	AGTCTGGGTC	GGCAAGACCG′gtgagtcgtc
2	57	1,069,318–1,069,374	1153	tgacgtgcag′CACTGGTGGT	AGAAATGCAG′gtgagacaat
3	77	1,070,528–1,070,604	780	gccttcatag′GTAATCTCTA	AGGTATTCAG′gtgagaagct
4	1,495	1,071,385–1,072,879	–	tctctttcag′GTCCATGAGA	TCGCATTTGA
4a	299	1,071,385–1,071,683	–	tctctttcag′GTCCATGAGA	ATGTCTACAG

Sequences of the two RASL11B transcripts identified in this study have been published in the GenBank database with the accession nos. AY839725 and AY839726.
[a] Derived from the current GenBank *Homo sapiens* genomic DNA reference sequence of chromosome 4 (NT_022853.14).

A

```
agtctgggtctggagcctgagccctgcggaacctcggcgctcggccccaccccgcccgtacctgcacttatttattgttgttatttcttaccgcggagcc  100
ccgcagtcgggtcctcccgcccgctcccgcgcagcgctagcattctccagtccctcagtcccttcccgcgcggtgcgccgcagccgaggcgATGCGCCTC  200
                                                                                    M  R  L    3
ATTCAGAACATGTGCACCATCGCCGAGTACCCCGCGCCGGGCAACGCCGCGGCCTCCGACTGCTGTGTGGGCGCCGCCGGCCGCCGCCTGGTCAAGATCG  300
 I  Q  N  M  C  T  I  A  E  Y  P  A  P  G  N  A  A  A  S  D  C  C  V  G  A  A  G  R  R  L  V  K  I     36
CCGTGGTGGGCGCCAGCGGCGTGGGCAAGACCGCACTGGTGGTCCGGTTCCTCACCAAACGATTCATCGGTGACTATGAAAGAAATGCAGGTAATCTCTA  400
A  V  V  G  A  S  G  V  G  K  T  A  L  V  V  R  F  L  T  K  R  F  I  G  D  Y  E  R  N  A  G  N  L  Y    70
TACTAGACAAGTTCAGATAGAAGGTGAAACCCTGGCTCTTCAGGTTCAAGACACTCCAGGTATTCAGGTCCATGAGAACAGCCTGAGCTGCAGTGAACAG  500
  T  R  Q  V  Q  I  E  G  E  T  L  A  L  Q  V  Q  D  T  P  G  I  Q  V  H  E  N  S  L  S  C  S  E  Q    103
CTGAATAGGTGCATTCGCTGGGCAGATGCTGTGGTGATCGTTTTCTCCATCACTGACTACAAGAGCTATGAACTCATCAGCCAGCTCCACCAGCACGTGC  600
 L  N  R  C  I  R  W  A  D  A  V  V  I  V  F  S  I  T  D  Y  K  S  Y  E  L  I  S  Q  L  H  Q  H  V     136
AGCAGCTACACCTGGGCACCCGGCTGCCTGTGGTGGTCGTGGCCAACAAAGCTGACCTGTTGCACATCAAACAGGTTGACCCTCAGCTTGGACTGCAGCT  700
Q  Q  L  H  L  G  T  R  L  P  V  V  V  V  A  N  K  A  D  L  L  H  I  K  Q  V  D  P  Q  L  G  L  Q  L    170
AGCCAGCATGCTAGGCTGCTCATTCTATGAAGTGTCTGTCAGTGAAAATTATAATGATGTCTACAGCGCCTTCCACGTCCTCTGTAAAGAGGTCAGTCAC  800
  A  S  M  L  G  C  S  F  Y  E  V  S  V  S  E  N  Y  N  D  V  Y  S  A  F  H  V  L  C  K  E  V  S  H    203
AAACAGCAGCCTAGCAGTACACCCGAGAAGCGAAGAACCTCCCTCATTCCCAGGCCCAAGTCACCCAACATGCAGGACCTGAAGAGGAGGTTTAAGCAAG  900
 K  Q  Q  P  S  S  T  P  E  K  R  R  T  S  L  I  P  R  P  K  S  P  N  M  Q  D  L  K  R  R  F  K  Q     236
CCCTCTCTGCCAAAGTGAGGACTGTCACCTCCGTCTGAagcaggaggagcactcaaggggttggtcttcccaggaagagggcctgaggttctcctagt 1000
A  L  S  A  K  V  R  T  V  T  S  V  *                                                                 244
gcaggaacgttgaatattggcaatgattcctggttccagaaagggctggagcagaagggccaagagggcctgtggaactgctacagaaaaggaagtgttg 1100
ttctgagcaggggacaggattgatgaggcttgaaagagcccactgagccactctctgaatatgtgaaatgtactctgtgtctttttcctttagagtgggg 1200
aggggggcataatcgtttcggtttctgcattcaactaccttgtaaatggtggtccgttgcagtttcaccaaatgtattgatgtgatttacagtgggaatga 1300
aagaacagattaagcattgataggctttctttttttccccctttttttctttttctctttctttctttttcctcttttttccccaagaggaagaattgc 1400
ttttctcttaccagtatgatttgtaactctggaacactattcttacagaatgcctttctaacctgaaggatacccagatttctttctttatgtacaagat 1500
ggaaaatcccctaccccctcaaaaacaggttgagtttatgggccagaatattttgtataccagacattggtaagctctcatggtttacaggaaggctctgg 1600
ttccccctcacaggatgagcatgctcagttgggcgtgtgtggaggagctgtgaacttcacgctcttcaaccccagactttgactgtatagttttttgttt 1700
ttttaactgttccatcaggaaaaaaatgtgtcagttgattttggtgtgacttgtgtaaatggttcatggcaatgacgttgggttgcttcctaggcctggc 1800
tgagttgtgcctaagggtggctgaaatactaaaacacttatcttacagcaagtgaacaggggctacctgccacatccctccacagatgcactttaaaaa 1900
gccactcatgctttggcttaaactgtaattaatttattttatgtacaataaatcgcatttgaaaaaaaaaa                               1962
```

B

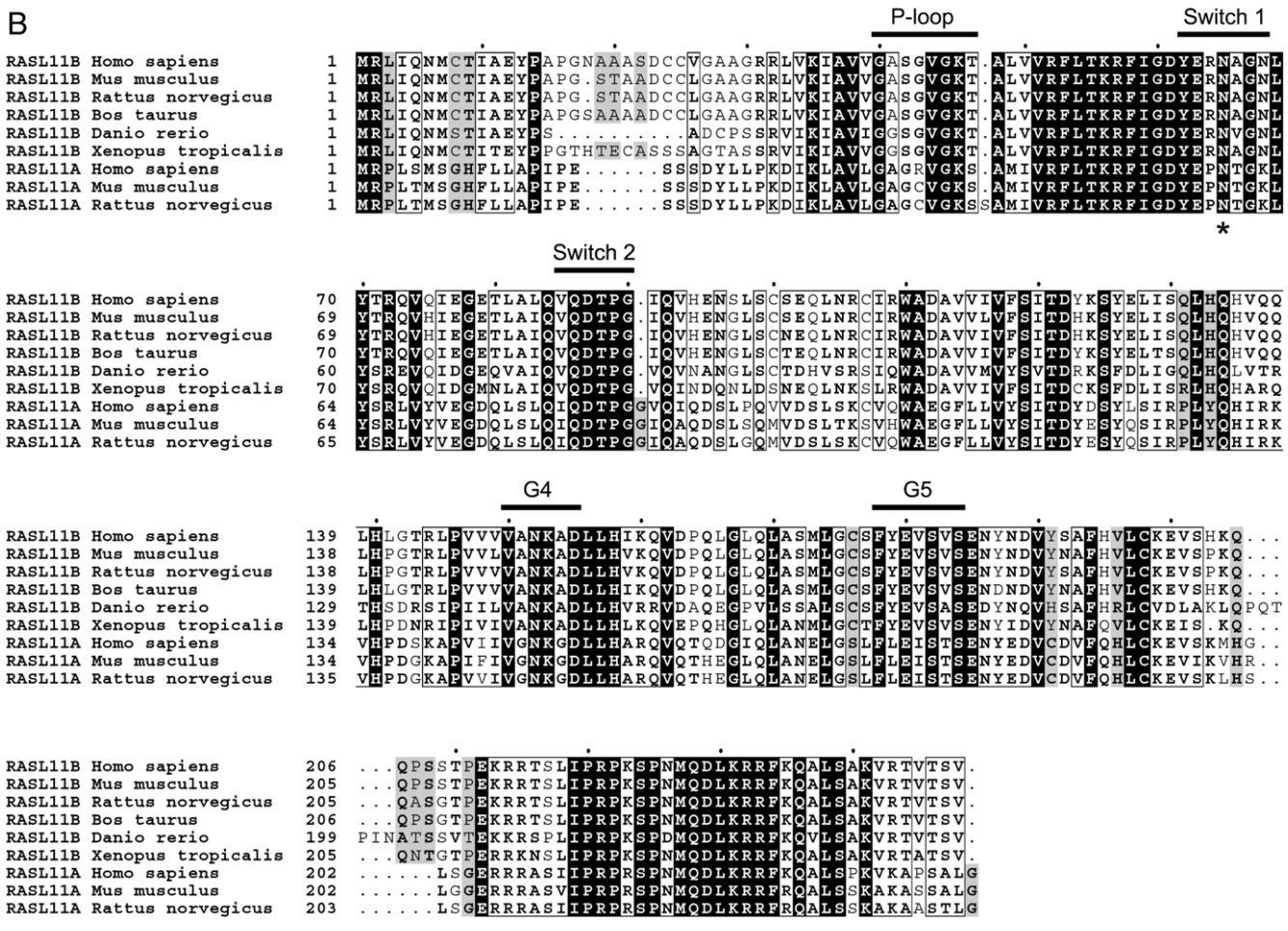

C

	RASL11A Hs	RASL11A Mm	RASL11A Rn	RASL11B Hs	RASL11B Mm	RASL11B Rn	RASL11B Bt	RASL11B Dr	RASL11B Xt
RASL11A Hs		93	91	74	75	75	74	67	73
RASL11A Mm	89		92	71	73	73	71	65	71
RASL11A Rn	87	90		75	76	75	74	68	75
RASL11B Hs	54	51	54		97	96	98	79	86
RASL11B Mm	54	51	54	94		99	96	79	86
RASL11B Rn	54	51	54	94	97		96	78	86
RASL11B Bt	53	50	53	95	94	95		78	84
RASL11B Dr	45	43	45	63	64	64	63		75
RASL11B Xt	54	53	55	73	75	75	74	61	

Similarity

Identity

Fig. 2. Sequence of RASL11B mRNA and protein, and homology between members of the RASL11 protein family. (A) Nucleic acid sequence and predicted amino acid sequence of human wild-type RASL11B. The mRNA sequence containing the open reading frame is shown in uppercase letters whereas the 5′- and 3′-untranslated region is shown in lowercase letters. Positions of the start codon (ATG) and stop codon (TGA) are printed in bold upper case letters. A polyadenylation signal within the mRNA sequence is highlighted in bold lowercase letters. Splice sites are indicated using a 'ᒣ'. A site of alternate polyadenylation is marked with '$^{\downarrow}_{AAAAAAAAAA}$'. The amino acid sequence is shown in upper case letters below the nucleic acid sequence. The conserved domain of the RAS protein family (Pfam accession no. PF00071) is highlighted using bold italic letters. The predicted RASL11B protein sequence of 248 amino acids is identical to GenBank entry NP_076429. (B) ClustalW alignment of the RASL11B and RASL11A homologous proteins contained in the GenBank RefSeq database. Only NCBI reference sequences of proteins with experimental evidence (according to the NCBI RefSeq sequence entry) which are homologous to RASL11B and RASL11A were used (predicted sequences were excluded). Amino acids are shown in single letter code; gaps due to alignment are represented by dots. Identical amino acids of all homologues are displayed with black background, residues which are conserved within the RASL11B or RASL11A group, respectively, but are not conserved from one group to the other are highlighted with grey background. Similar amino acid residues are boxed. The five conserved regions that contribute to the G-domain of small GTPases are indicated with bars. An asparagine residue in the switch 1 motif is indicated with an asterisk. This residue is conserved within the RASL11 protein family but in other RAS-like small GTPases this amino acid is replaced by threonine [7]. This threonine residue has been suggested to be important for stabilizing the GTP-bound form. Thus, it is likely that the asparagine substitution at this position affects the molecular function of the RASL11 proteins. (C) Grade of identity and similarity of experimentally validated RASL11 proteins in the GenBank RefSeq database in percent. Grade of identity and similarity at the protein level were calculated using the NCBI BLAST 2 Sequences tool using standard settings without using the filter function (http://www.ncbi.nlm.nih.gov/blast/bl2seq/bl2.html). The following GenBank database entries were used: *Homo sapiens* RASL11B, NP_076429; *Mus musculus* RASL11B, NP_081154; *Rattus norvegicus* RASL11B, NP_001002830; *Bos taurus* RASL11B, NP_001015635; *Danio rerio* RASL11B, NP_956434; RASL11B, *Xenopus tropicalis* NP_001015774; *Homo sapiens* RASL11A, NP_996563; *Mus musculus* RASL11A, NP_081140, and *Rattus norvegicus* RASL11A, NP_001002829. The following abbreviations are used: Bt, *Bos taurus*; Dr, *Danio rerio*; Hs, *Homo sapiens*; Mm, *Mus musculus*; Rn, *Rattus norvegicus*; Xt, *Xenopus tropicalis*.

predictive for a cytoplasmic localization (57% probability) according to the *k*-nearest neighbors classifier algorithm [33]. In agreement to this prediction, RASL11B has no prenylation signal according to PrePS (Prenylation Prediction Suite; http://mendel.imp.ac.at/sat/PrePS/index.html), indicating that this protein is probably not anchored to cellular membranes. The RASL11B splice variant encodes a putative protein of 191 amino acids. According to SMART, the shorter RASL11B variant still contains a characteristic small GTPase domain but it lacks the 57 amino acids of the C-terminus of the RASL11B wild-type transcript which are highly conserved within the RASL11 protein family (see Supplemental Data).

3.3. Putative regulatory elements in the core promoter

The core promoter of the human *RASL11B* gene immediately upstream of exon 1 was analyzed using TESS, MatInspector and Mapper to identify potentially regulatory elements and transcription factor binding sites. These analyses revealed that the region from the transcription start site to −2000 bp upstream has a G/C content of 51%, lacks a TATA box within the first 100 nucleotides upstream of the transcription start site, but is predicted to contain a CCAAT box and several Sp1 binding sites within the first 200 bp. Sp1 and CCAAT binding proteins are ubiquitously expressed and constitutively activate the transcription of genes. They have not been, by themselves, implicated in changing the rates of individual gene transcription in a chromosomal context [34]. Mapper, MatInspector and TESS analyses revealed no binding sites known to be involved in TGF-β1 signaling, but a serum response factor (SRF) site was predicted at position −441. The transcription factor SRF activates genes involved in smooth muscle cell differentiation and proliferation by recruiting muscle-restricted cofactors and is both induced and activated by TGF-β1 [35–37].

3.4. Identification of homologous proteins

The formatted CLUSTALW alignment revealed a high similarity between the RASL11A and RASL11B proteins within the conserved RAS domain (Fig. 2B). Grade of identity and similarity of RASL11 proteins in percent of the above mentioned homologous proteins are shown in Fig. 2C. The

sequence identity between the human RASL11B and the human RASL11A amounts 54% and the similarity 74%.

3.5. Phylogenetic tree

The evolution of the RASL11 family is displayed in Fig. 3. RASL11A, RASL11B and RASL11C form subfamilies (shorthand A, B, C) probably due to duplication of an ancestral gene. With few exceptions, the subfamilies follow species phylogeny as can be checked with TreeSimplifier [38] or by manual comparison with a standard species tree [NCBI taxonomy; [39,40]]. In subfamily A, the dog and the rabbit sequences do not fit, but corresponding subtrees have small bootstrap support (55% and 42%, respectively). In subfamily B, the same phenomenon occurs (bootstrap support 34% and 42%, respectively). Furthermore, mouse and rat sequences of subfamily B feature the frequently occurring dis-association with the primate sister lineage, presumably due to the fast evolution of rodents in comparison to primates [41–43]. The high congruence of gene and species tree indicates that no further duplications of any subfamily occurred, and there is no notable evidence for duplications with subsequent losses leading to hidden paralogy [44]. In other words, no birth and death processes are observed as for, for example, ATP-binding cassette transporters [16]. Such a stable situation is particularly noteworthy for fish, which usually feature a lot of gene duplications. Suppression of the survival of duplicates of a gene may be explained by the importance of the dosage (expression level) of the gene in question [45]; if dosage is important, any paralogs are rapidly wiped out (they become pseudogenes or get lost altogether) if their continued expression leads to an imbalance in metabolism or regulation. As will be described below, expression analysis of RASL11A and RASL11B reveals that dosage is important for these genes since their expression is anti-correlated at least in some situations. Based on the data available, the placental mammals have lost the C subfamily which may not be an essential part of the relationship of RASL11B and RASL11A.

3.6. Conserved motifs

The VisCoSe alignment of the RASL11 proteins shown in the phylogenetic tree in Fig. 3 revealed that the protein sequence of the entire RASL11 protein family is highly conserved within different species (see Supplemental Data). Nevertheless, each subfamily has several amino acid residues which are conserved within the subfamily. The degree of conservation within each subfamily and the entire RASL11 protein family is obvious if a reduced amino acid alphabet is used that reduces the complexity in protein sequences by sorting amino acids with similarities into groups (see Supplemental Data) [46].

3.7. Tissue-specific expression

We analyzed tissue-specific expression of the wild-type RASL11B and RASL11A transcripts using real-time RT-PCR with total RNA obtained from 37 different human tissues and five different human cell types (Fig. 4). In the different tissues, the RASL11B transcript was most abundant in placenta (more than 900-fold expressed compared to bone marrow) followed by spleen (232-fold), kidney (220-fold), brain (201-fold), ovary (204-fold) and uterus (171-fold). In the cell types the RASL11B transcript had the highest abundance in primary macrophages (Fig. 4A). RASL11A showed an expression pattern different from that of RASL11B (Fig. 4B). Expression of RASL11A showed highest levels in colon tumor and normal colon tissue (320- and 257-fold, respectively) followed by small intestine (173-fold), liver (167-fold), jejunum (133-fold), ileum (132-fold), bladder (111-fold), and aorta (108-fold). Lowest expression of RASL11A was observed in endothelial cells.

3.8. Expression of RASL11B is induced by TGF-β1

We have recently shown that TGF-β1 induces the expression of the small Rab GTPase interacting factor SMAP-5 [11]. Furthermore, the promoter of RASL11B is predicted to contain an SRF binding site, and SRF is known to be induced and activated by TGF-β1 [35–37]. To test whether TGF-β1 modulates the expression of the small RAS-like GTPases RASL11B and RASL11A, we analyzed expression of RASL11B and RASL11A in human caSMCs treated with 10 ng/ml TGF-β1 for different times as indicated in Fig. 5. As shown in Fig. 5A, TGF-β1 induced RASL11B expression in a time-dependent manner. Up-regulation achieved a maximum at 8 h and was statistically significant after 2 h (6.2 ± 3.1; $p < 0.05$), 4 h (23.6 ± 10.2; $p < 0.01$), 8 h (29.0 ± 12.8; $p < 0.01$), and 24 h (12.7 ± 8.8; $p < 0.05$). By contrast, TGF-β1 decreased expression of the RASL11B homologue RASL11A in a time-dependent manner (Fig. 5B). Down-regulation achieved a minimum at 8 h and was statistically significant after 2 h (0.5 ± 0.3; $p < 0.01$), 4 h (0.5 ± 0.1; $p < 0.01$), and 8 h (0.3 ± 0.5; $p < 0.01$).

3.9. Expression of RASL11B is increased during maturation of THP-1 monocytes into macrophages

TGF-β1 promotes differentiation of the human promonocytic THP-1 leukemia cell line [47], and expression of TGFB1 and TGFBR2 mRNAs is increased during phorbol 12-myristate 13-acetate-induced differentiation of THP-1 monocytes into macrophages [48]. This raised the question how macrophage maturation influences expression of RASL11A and RASL11B. We therefore investigated the expression of both genes during phorbol 12-myristate 13-acetate-induced maturation of monocytes of the human THP-1 leukemia cell line into macrophages. Real-time RT-PCR analyses revealed that the expression of RASL11B mRNA is induced more than ninefold within 6 days of phorbol ester-induced maturation of THP-1 monocytes (7.1 ± 1.5 fold after 4 days, $p < 0.01$; 9.8 ± 7.3 fold after 6 days, $p < 0.01$; Fig. 6A). In contrast, expression of RASL11A mRNA decreased about tenfold during the differentiation of THP-1 monocytes into macrophages (0.6 ± 0.1 fold after 4 days, $p < 0.01$; 0.1 ± 0.1 fold after 6 days, $p < 0.01$; Fig. 6B). Preliminary real-time RT-PCR expression analyses were performed using primary

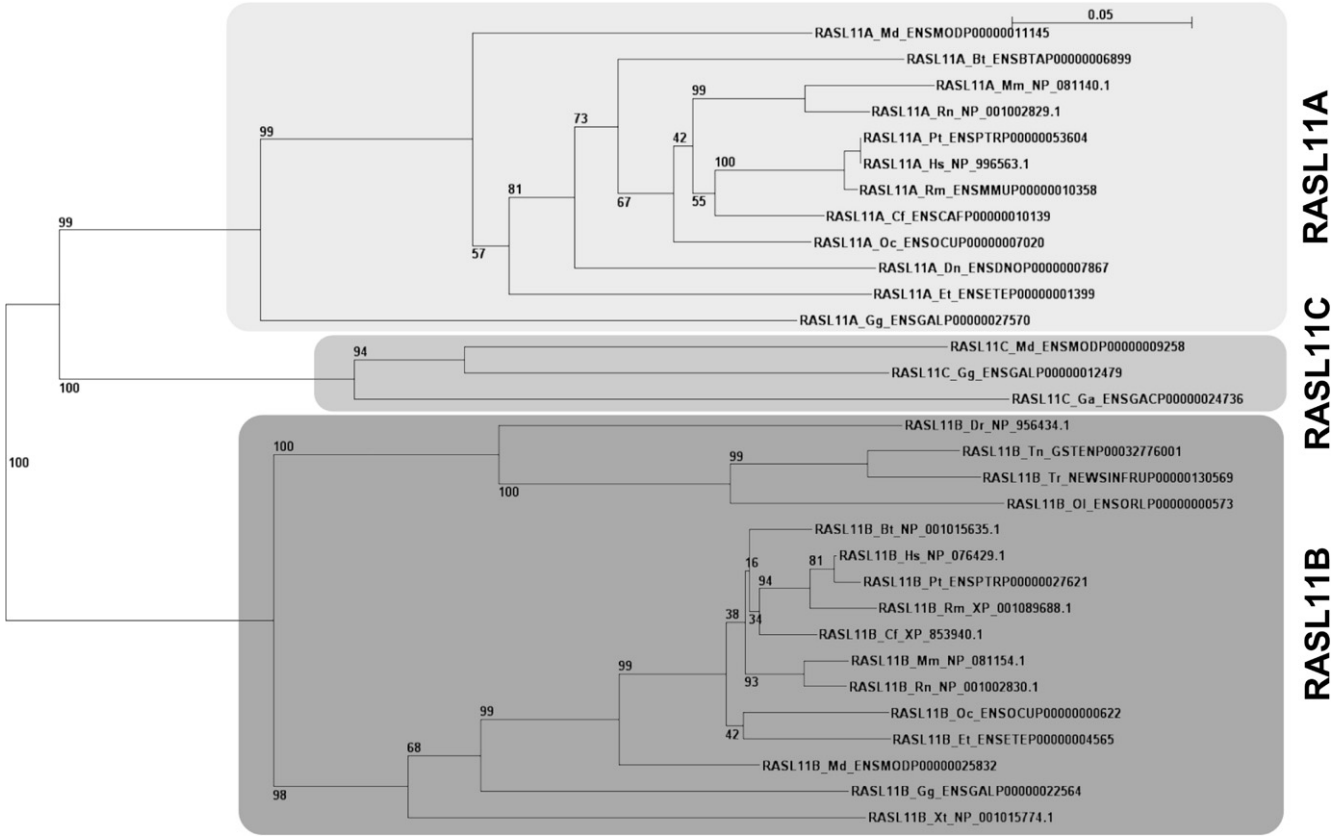

Fig. 3. Gene phylogeny of the RASL11 family. RASL11A, RASL11B and RASL11C form subfamilies (shorthand A, B, C). With few exceptions, the subfamilies follow species phylogeny. The following abbreviations were used: Bt, *Bos taurus* (cattle, Hereford breed); Cf, *Canis familiaris* (dog); Dn, *Dasypus novemcinctus* (nine-banded, long-nosed armadillo); Dr, *Danio rerio* (zebrafish); Et, *Echinops telfairi* (small Madagascar hedgehog); Ga, *Gasterosteus aculeatus* (three-spined stickleback); Gg, *Gallus gallus* (chicken); Hs, *Homo sapiens*; La, *Loxodonta africana* (African bush elephant); Md, *Monodelphis domestica* (gray short-tailed opossum); Mm, *Mus musculus* (house mouse); Oc, *Oryctolagus cuniculus* (European rabbit); Ol, *Oryzias latipes* (Japanese medaka or Japanese killifish); Pt, *Pan troglodytes* (common chimpanzee); Rm, *Macaca mulatta* (rhesus monkey); Rn, *Rattus norvegicus* (brown rat); Tn, *Tetraodon nigroviridis* (green spotted puffer); Tr, *Takifugu rubripes* (fugu, pufferfish); Xt, *Xenopus tropicalis* (Western clawed frog).

monocytes and primary monocyte-derived macrophages obtained from two individuals. During the differentiation of the human primary monocytes into mature macrophages within 14 days, the expression of RASL11B mRNA increased between about 20- and 200-fold during the 14 days of maturation of human primary monocytes confirming our findings in THP-1 cells (data not shown).

4. Discussion

We cloned for the first time the full-length human RASL11B transcript and identified a single shorter splice variant. The physiological importance of the splice variant is unclear. The identification of the 5′-end of the RASL11B mRNA allowed us to analyze the core promoter of the human *RASL11B* gene *in silico*. The core promoter contains GC box elements (Sp1 sites) and lacks a TATA box as is typical for promoters of ubiquitously expressed proteins. Consistent with this, RASL11B was expressed in all analyzed tissues. Nevertheless, the expression of RASL11B varies up to about 900-fold among the human tissues and cell types tested. Highest levels of expression were found in placenta, spleen, kidney, ovary, brain, uterus, testis, and cultured primary macrophages. This suggests that additional transacting factors may be involved in tissue- or cell-type-specific expression of RASL11B.

The protein encoded by the *RASL11B* gene seems to be a small RAS-like GTPase lacking characteristics of other RAS proteins such as prenylation sites [5,6]. This is in accordance with *in silico* analyses predicting a cytoplasmic localization of the RASL11B protein. A comparison of the RASL11 protein sequences obtained from different species revealed a high degree of conservation within the entire RASL11 protein family.

To get insights into the function of RASL11B we analyzed expression of RASL11B and of its closest human homologue RASL11A during maturation of human monocytes into macrophages and in human coronary artery smooth muscle cells in response to TGF-β1. Both processes play an important role in atherogenesis [11,49]. In the atherosclerotic vessel wall, macrophages are a major source of TGF-β1, thus stimulating neighboring smooth muscle cells to produce, for example, extracellular matrix molecules [49].

Phorbol ester-induced maturation of THP-1 monocytes into macrophages has opposite effects on the expression of RASL11B (up-regulation) and RASL11A (down-regulation).

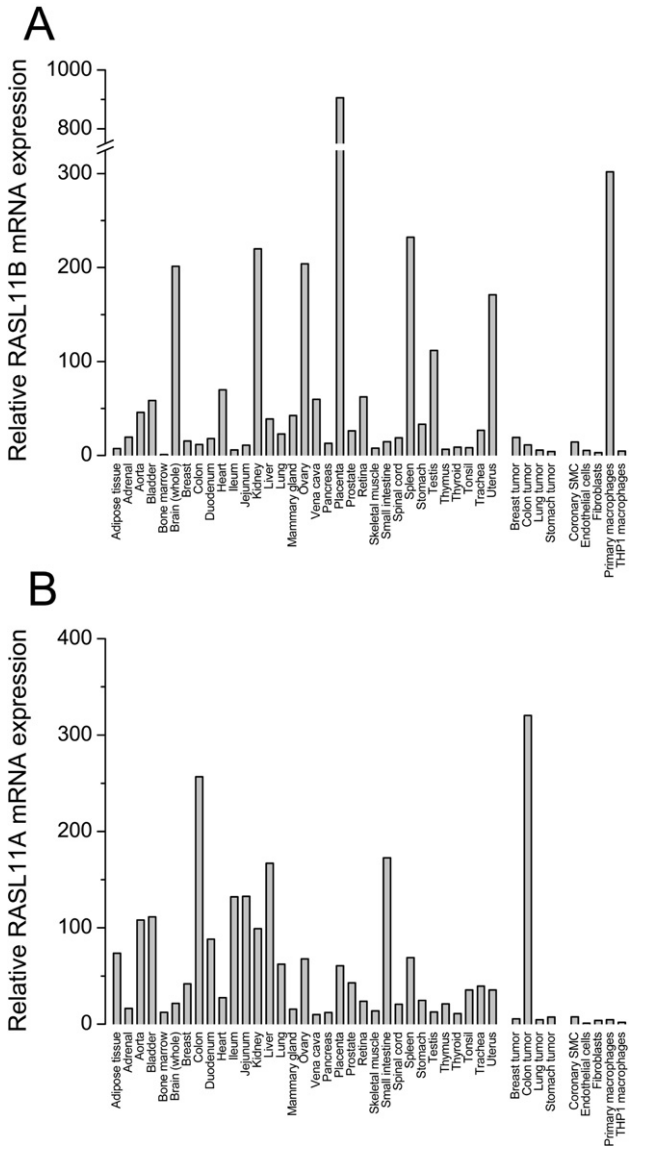

Fig. 4. RASL11B expression in different tissues and cultured cells as measured by real-time RT-PCR analyses. (A) Fold changes were calculated using RASL11B mRNA expression in bone marrow as reference. In cultured cells, highest RASL11B expression was detected in primary macrophages. In tissues, highest levels of RASL11B mRNA were found in placenta, spleen, kidney, brain, ovary, and uterus. (B) RASL11A expression was different compared to that of RASL11B. Expression of RASL11A showed highest levels in colon tumor and normal colon tissue and was high in small intestine, liver, jejunum, ileum, bladder, and aorta. Cultured cells showed relatively low expression of RASL11A. In both cases, expression values were normalized to the geometric mean of the most stably expressed housekeeping genes 14 kDa signal recognition particle, H3 histone family 3A and DNA directed RNA polymerase II polypeptide K.

The same pattern of regulation was observed in human coronary artery smooth muscle cells in response to TGF-β1. The finding that RASL11B and RASL11A were regulated in opposite directions, both with the highest regulation 8 h after treatment with TGF-β1, indicate that the expression of both genes is likely regulated by the same pathway and that the encoded gene products RASL11B and RASL11A may have opposite functions.

The mechanisms behind the regulation of RASL11B and RASL11A expression during TGF-β1 stimulation of coronary artery smooth muscle cells are yet not clear. It is likely that TGF-β1 induces RASL11B expression in coronary artery smooth muscle cells via the transcription factor SRF. The RASL11B promoter contains a SRF binding site and in myofibroblasts it was shown that TGF-β1 induces and activates SRF, thus inducing expression of SRF target genes [35–37]. How expression of RASL11B and RASL11A is regulated during macrophage maturation is also not clear. It has been shown that there is minimal TGF-β1 secretion by unactivated monocytes whereas mature and activated macrophages secrete TGF-β1 [50]. Thus, the increase in RASL11B expression during macrophage maturation may occur as a consequence of increased TGF-β1 secretion. However, further studies are required to test these hypotheses.

So far, nothing is known about the physiological role of RASL11B. The closest human homologue of RASL11B is

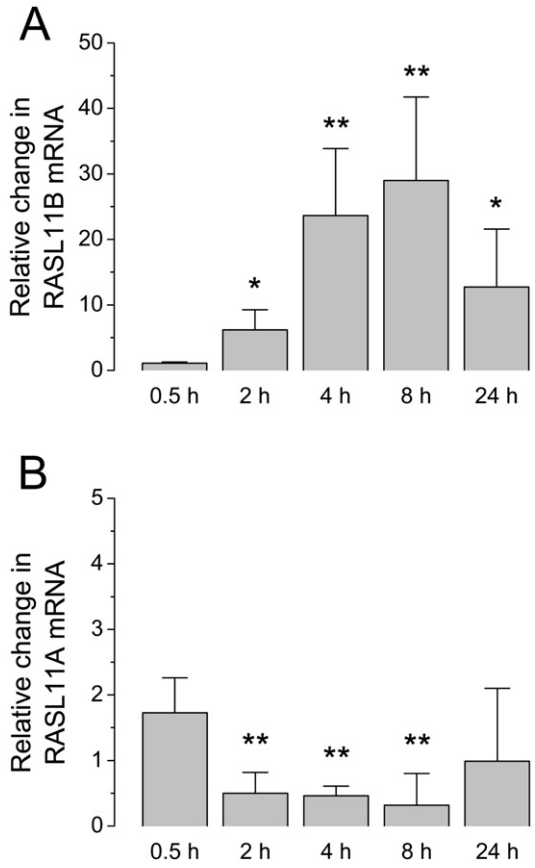

Fig. 5. Time-dependent regulation of RASL11B and RASL11A mRNA expression in human vascular smooth muscle cells treated with 10 ng/ml transforming growth factor-β1 (TGF-β1) as measured by real-time RT-PCR analyses. (A) RASL11B mRNA was significantly up-regulated after 2 h (6.2±3.1; $p<0.05$), 4 h (23.6±10.2; $p<0.01$), 8 h (29.0±12.8; $p<0.01$), and 24 h (12.7±8.8; $p<0.05$). Cells not treated with TGF-β1 were used as reference. Fold changes were calculated to control cells and normalized to mRNA levels of the 14 kDa signal recognition particle (SRP14), expression of which was not affected by TGF-β1 (not shown). (B) RASL11A mRNA was significantly down-regulated after 2 h (0.5±0.3; $p<0.01$), 4 h (0.5±0.1; $p<0.01$), and 8 h (0.3±0.5; $p<0.01$). Symbols used are: *$p<0.05$; **$p<0.01$.

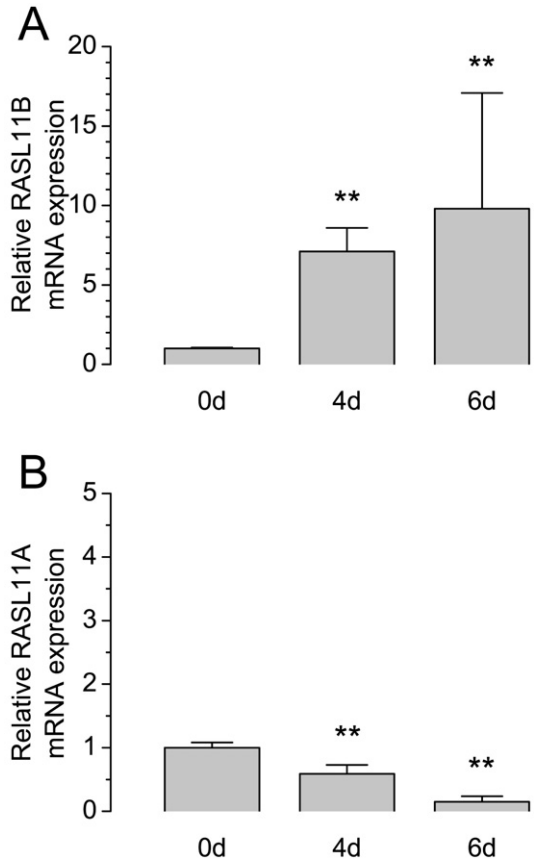

Fig. 6. Expression of RASL11B and RASL11A during THP-1 maturation. (A) Expression of RASL11B was up-regulated during phorbol ester-induced maturation of THP-1 monocytes into macrophages (7.1±1.5 fold after 4 days, $p<0.01$; 9.8±7.3 fold after 6 days, $p<0.01$). (B) By contrast, expression of RASL11A was down-regulated during phorbol ester-induced maturation of THP-1 cells into macrophages (0.6±0.1 fold after 4 days, $p<0.01$; 0.1±0.1 fold after 6 days, $p<0.01$). Fold changes were calculated to control cells and normalized to mRNA levels of the 14-kDa signal recognition particle (SRP14).

RASL11A, which was first cloned and described by Louro et al. [7]. The authors of this study hypothesized that RASL11A, which was shown to be down-regulated in prostate tumors, may have a tumor suppressor role in prostate cancer, but no experimental data supporting this hypothesis is available. In the tumor tissues investigated in our study, expression of RASL11B was similar or slightly lower compared to that in normal tissues. However, no data is available supporting a functional role of RASL11B in tumor development.

Further studies are required to elucidate the physiological importance of RASL11B for macrophage maturation and TGF-β1 signaling processes. Nevertheless, because RASL11B is involved in TGF-β1-mediated processes, it may play a role in development or disease conditions such as inflammation, cancer, and arteriosclerosis.

Acknowledgements

We thank Thomas Böking and Christine Fabritius for their excellent technical assistance. We are also thankful to Jürgen Rauterberg for critical comments and helpful discussion. The study was supported by the Deutsche Forschungsgemeinschaft and the European Union [51].

Appendix A. Supplementary data

Supplementary data associated with this article can be found, in the online version, at doi:10.1016/j.bbaexp.2007.05.005.

References

[1] B.R. Ali, M.C. Seabra, Targeting of Rab GTPases to cellular membranes, Biochem. Soc. Trans. 33 (2005) 652–656.
[2] Y. Takai, T. Sasaki, T. Matozaki, Small GTP-binding proteins, Physiol. Rev. 81 (2001) 153–208.
[3] K. Wennerberg, K.L. Rossman, J.D. Channing, The RAS superfamily at a glance, J. Cell Sci. 118 (2005) 843–846.
[4] I.R. Vetter, A. Wittinghofer, The guanine nucleotide-binding switch in three dimensions, Science 294 (2001) 1299–1304.
[5] L.P. Wright, M.R. Philips, Lipid posttranslational modifications, CAAX modification and membrane targeting of Ras, J. Lipid Res. 47 (2006) 883–891.
[6] G.W. Reuther, C.J. Der, The Ras branch of small GTPases: Ras family members don't fall far from the tree, Curr. Opin. Cell Biol. 12 (2000) 157–165.
[7] R. Louro, H.I. Nakaya, A.C. Paquola, E.A. Martins, A.M. da Silva, S. Verjovski-Almeida, E.M. Reis, RASL11A, member of a novel small monomeric GTPase gene family, is down-regulated in prostate tumors, Biochem. Biophys. Res. Commun. 316 (2004) 618–627.
[8] K. Stolle, B. Weitkamp, J. Rauterberg, S. Lorkowski, P. Cullen, Laser microdissection-based analysis of mRNA expression in human coronary arteries with intimal thickening, J. Histochem. Cytochem. 52 (2004) 1511–1518.
[9] S. Lorkowski, S. Rust, T. Engel, E. Jung, K. Tegelkamp, E.A. Galinski, G. Assmann, P. Cullen, Genomic sequence and structure of the human ABCG1 (ABC8) gene, Biochem. Biophys. Res. Commun. 280 (2001) 121–131.
[10] S. Lorkowski, M. Kratz, C. Wenner, R. Schmidt, B. Weitkamp, M. Fobker, J. Reinhardt, J. Rauterberg, E.A. Galinski, P. Cullen, Expression of the ATP-binding cassette transporter gene ABCG1 (ABC8) in Tangier disease, Biochem. Biophys. Res. Commun. 283 (2001) 821–830.
[11] K. Stolle, M. Schnoor, G. Fuellen, M. Spitzer, T. Engel, F. Spener, P. Cullen, S. Lorkowski, Cloning, cellular localization, genomic organization, and tissue-specific expression of the TGFbeta1-inducible SMAP-5 gene, Gene 351 (2005) 119–130.
[12] J. Vandesompele, K. De Preter, F. Pattyn, B. Poppe, N. Van Roy, A. De Paepe, F. Speleman, Accurate normalization of real-time quantitative RT-PCR data by geometric averaging of multiple internal control genes, Genome Biol. 3 (2002) RESEARCH0034.
[13] B. Morgenstern, DIALIGN 2: improvement of the segment-to-segment approach to multiple sequence alignment, Bioinformatics 15 (1999) 211–218.
[14] M. Spitzer, G. Fuellen, P. Cullen, S. Lorkowski, VisCoSe: visualization and comparison of consensus sequences, Bioinformatics 20 (2004) 433–435.
[15] G. Fuellen, M. Spitzer, P. Cullen, S. Lorkowski, BLASTing proteomes, yielding phylogenies, In Silico Biol. 3 (2003) 313–319.
[16] G. Fuellen, M. Spitzer, P. Cullen, S. Lorkowski, Correspondence of function and phylogeny of ABC proteins based on an automated analysis of 20 model protein data sets, Proteins 61 (2005) 888–899.
[17] S.F. Altschul, T.L. Madden, A.A. Schäffer, J. Zhang, Z. Zhang, W. Miller, D.J. Lipman, Gapped BLAST and PSI-BLAST: a new generation of protein database search programs, Nucleic Acids Res. 25 (1997) 3389–3402.
[18] K. Katoh, K. Kuma, H. Toh, T. Miyata, MAFFT version 5: improvement in accuracy of multiple sequence alignment, Nucleic Acids Res. 33 (2005) 511–518.
[19] K. Howe, A. Bateman, R. Durbin, QuickTree: building huge Neighbour-Joining trees of protein sequences, Bioinformatics 18 (2002) 1546–1547.

[20] J.P. Huelsenbeck, F. Ronquist, MRBAYES: Bayesian inference of phylogenetic trees, Bioinformatics 17 (2001) 754–755.
[21] F. Ronquist, J.P. Huelsenbeck, MrBayes 3: Bayesian phylogenetic inference under mixed models, Bioinformatics 19 (2003) 1572–1574.
[22] A. Stamatakis, RAxML-VI-HPC: maximum likelihood-based phylogenetic analyses with thousands of taxa and mixed models, Bioinformatics 22 (2006) 2688–2690.
[23] G. Perriere, M. Gouy, WWW-query: an on-line retrieval system for biological sequence banks, Biochimie 78 (1996) 364–369.
[24] H. Nielsen, J. Engelbrecht, S. Brunak, G. von Heijne, A neural network method for identification of prokaryotic and eukaryotic signal peptides and prediction of their cleavage sites, Int. J. Neural Syst. 8 (1997) 581–599.
[25] I. Letunic, L. Goodstadt, N.J. Dickens, T. Doerks, J. Schultz, R. Mott, F. Ciccarelli, R.R. Copley, C.P. Pontin, P. Bork, Recent improvements to the SMART domain-based sequence annotation resource, Nucleic Acids Res. 30 (2002) 242–244.
[26] K. Nakai, P. Horton, PSORT: a program for detecting sorting signals in proteins and predicting their subcellular localization, Trends Biochem. Sci. 24 (1999) 34–36.
[27] J. Schug, Using TESS to predict transcription factor binding sites in DNA sequence, in: A.D. Baxevanis, D.B. Davison, R.D.M. Page, G.A. Petsko, L.D. Stein, G.D. Stormo (Eds.), Current Protocols in Bioinformatics, John Wiley and Sons, New York, 2003.
[28] K. Cartharius, K. Frech, K. Grote, B. Klocke, M. Haltmeier, A. Klingenhoff, M. Frisch, M. Bayerlein, T. Werner, MatInspector and beyond: promoter analysis based on transcription factor binding sites, Bioinformatics 21 (2005) 2933–2942.
[29] V.D. Marinescu, I.S. Kohane, A. Riva, MAPPER: a search engine for the computational identification of putative transcription factor binding sites in multiple genomes, BMC Bioinformatics 6 (2005) 79.
[30] P. Gouet, X. Robert, E. Courcelle, ESPript/ENDscript: extracting and rendering sequence and 3D information from atomic structures of proteins, Nucleic Acids Res. 31 (2003) 3320–3323.
[31] R. Breathnach, P. Chambon, P, Organization and expression of eucaryotic split genes coding for proteins, Annu. Rev. Biochem. 50 (1981) 349–383.
[32] H. Stenmark, V.M. Olkkonen, The Rab GTPase family, Genome Biol. 2 (2001) REVIEWS3007.
[33] P. Horton, K. Nakai, Better prediction of protein cellular localization sites with the k nearest neighbors classifier, Proc. Int. Conf. Intell. Syst. Mol. Biol. 5 (1997) 147–152.
[34] A.H. Brivanlou, J.E. Darnell, Signal transduction and the control of gene expression, Science 295 (2002) 813–818.
[35] J. Chai, M. Norng, A.S. Tarnawski, J. Chow, A critical role of serum response factor in myofibroblast differentiation during experimental oesophageal ulcer healing in rats, Gut 56 (2007) 621–630.
[36] T. Ueyama, S. Kawashima, T. Sakoda, K. Hirata, Y. Ohashi, W. Yamochi, H. Akita, M. Yokoyama, Transforming growth factor-beta1 and protein kinase C synergistically activate the c-*fos* serum response element in myocardial cells, J. Mol. Cell. Cardiol. 30 (1998) 551–562.
[37] P. Qiu, X.H. Feng, L. Li, Interaction of Smad3 and SRF-associated complex mediates TGF-beta1 signals to regulate SM22 transcription during myofibroblast differentiation, J. Mol. Cell. Cardiol. 35 (2003) 1407–1420.
[38] P.L. Lott, M. Mundry, C. Sassenberg, S. Lorkowski, G. Fuellen, Simplifying gene trees for easier comprehension, BMC Bioinformatics 7 (2006) 231.
[39] D.L. Wheeler, T. Barrett, D.A. Benson, S.H. Bryant, K. Canese, V. Chetvernin, D.M. Church, M. DiCuccio, R. Edgar, S. Federhen, L.Y. Geer, Y. Kapustin, O. Khovayko, D. Landsman, D.J. Lipman, T.L. Madden, D.R. Maglott, J. Ostell, V. Miller, K.D. Pruitt, G.D. Schuler, E. Sequeira, S.T. Sherry, K. Sirotkin, A. Souvorov, G. Starchenko, R.L. Tatusov, T.A. Tatusova, L. Wagner, E. Yaschenko, Database resources of the National Center for Biotechnology Information, Nucleic Acids Res. 35 (2007) D5–D12.
[40] W.J. Murphy, E. Eizirik, W.E. Johnson, Y.P. Zhang, O.A. Ryder, S.J. O'Brien, Molecular phylogenetics and the origins of placental mammals, Nature 409 (2001) 614–618.
[41] A. Farwick, U. Jordan, G. Fuellen, D. Huchon, F. Catzeflis, J. Brosius, J. Schmitz, Automated scanning for phylogenetically informative transposed elements in rodents, Syst. Biol. 55 (2006) 936–948.
[42] D. Huchon, F.M. Catzeflis, E.J. Douzery, Variance of molecular datings, evolution of rodents and the phylogenetic affinities between Ctenodactylidae and Hystricognathi, Proc. Biol. Sci. 267 (2000) 393–402.
[43] J.O. Kriegs, G. Churakov, M. Kiefmann, U. Jordan, J. Brosius, J. Schmitz, Retroposed elements as archives for the evolutionary history of placental mammals, PLoS Biol. 4 (2006) e91.
[44] A.P. Martin, T.M. Burg, Perils of paralogy: using HSP70 genes for inferring organismal phylogenies, Syst. Biol. 51 (2002) 570–587.
[45] M. Lynch, J.S. Conery, The evolutionary fate and consequences of duplicate genes, Science 290 (2000) 1151–1155.
[46] T. Li, K. Fan, J. Wang, W. Wang, Reduction of protein sequence complexity by residue grouping, Protein Eng. 16 (2003) 323–330.
[47] C. Bombara, R.A. Ignotz, TGF-beta inhibits proliferation of and promotes differentiation of human promonocytic leukemia cells, J. Cell. Physiol. 153 (1992) 30–37.
[48] J. Taipale, S. Matikainen, M. Hurme, J. Keski-Oja, Induction of transforming growth factor beta 1 and its receptor expression during myeloid leukemia cell differentiation, Cell Growth Differ. 5 (1994) 1309–1319.
[49] N.N. Singh, D.P. Ramji, The role of transforming growth factor-beta in atherosclerosis, Cytokine Growth Factor Rev. 17 (2006) 487–499.
[50] R.K. Assoian, B.E. Fleurdelys, H.C. Stevenson, P.J. Miller, D.K. Madtes, E.W. Raines, R. Ross, M.B. Sporn, Expression and secretion of type beta transforming growth factor by activated human macrophages, Proc. Natl. Acad. Sci. U. S. A. 84 (1987) 6020–6024.
[51] S. Bellosta, F. Bernini, G. Chinetti, A. Cignarella, P. Cullen, A. von Eckardstein, A. Exley, J. Freeth, M. Goddard, M. Hofker, E. Kanters, P. Kovanen, S. Lorkowski, M. Pentikainen, J. Printen, J. Rauterberg, A. Ritchie, B. Staels, B. Weitkamp, M. de Winther, Macrophage function and stability of atherosclerotic plaque consortium, macrophage function and stability of the atherosclerotic plaque: progress report of a European project, Nutr. Metab. Cardiovasc. Dis. 12 (2002) 3–11.